Figures of Chapter 6, Li_2ZrO_3

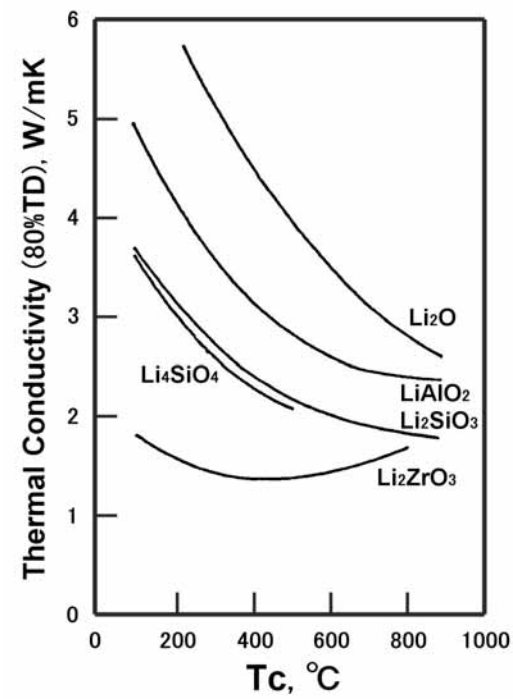

Fig.6.1 Thermal conductivity of Li_2ZrO_3, Li_2O and Li_4SiO_4 (80% TD). [17]

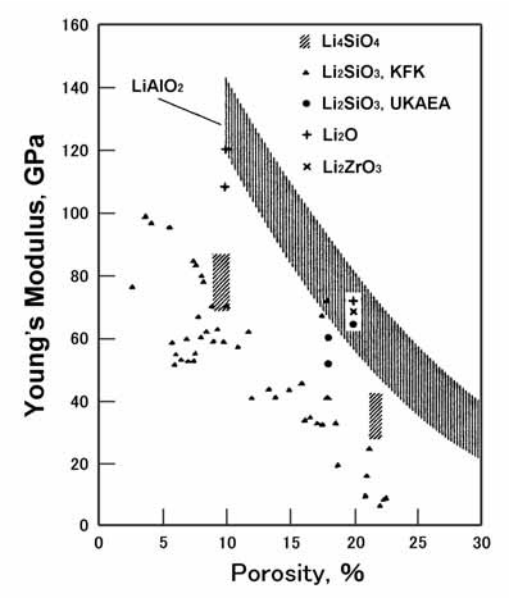

Fig.6.2 Porosity dependence of Young's Modulus values for Li_2ZrO_3, Li_2O and Li_4SiO_4. [50) 17) 6)]

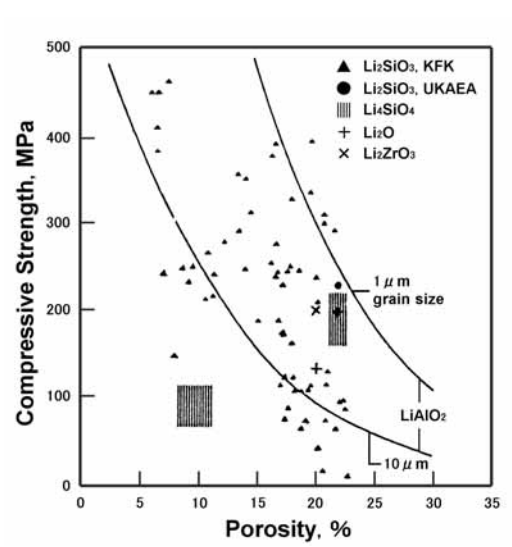

Fig.6.3 Porosity dependence of compressive strengths for Li_2ZrO_3, Li_2O and Li_4SiO_4. [17]

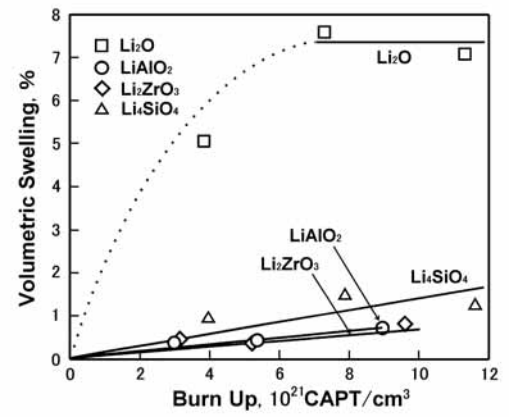

Fig.6.4 Volumetric swelling of Li_2ZrO_3, Li_2O and Li_4SiO_4 at 700℃. [49)]

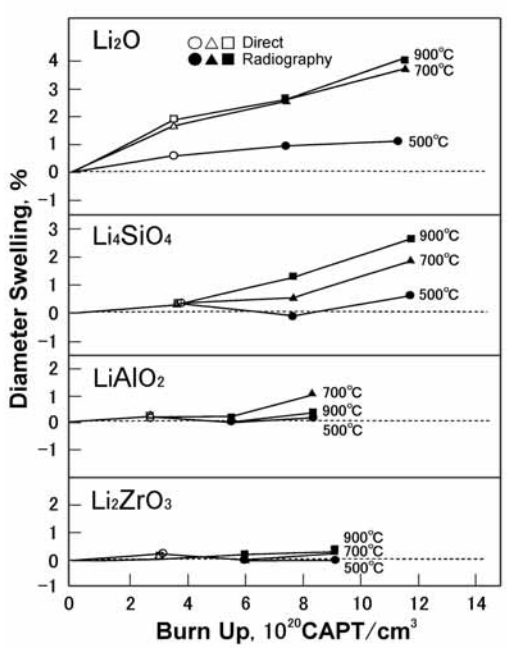

Fig.6.5 Diameter swelling of Li_2ZrO_3, Li_2O and Li_4SiO_4 at 500℃, 700℃, 900℃. [70]

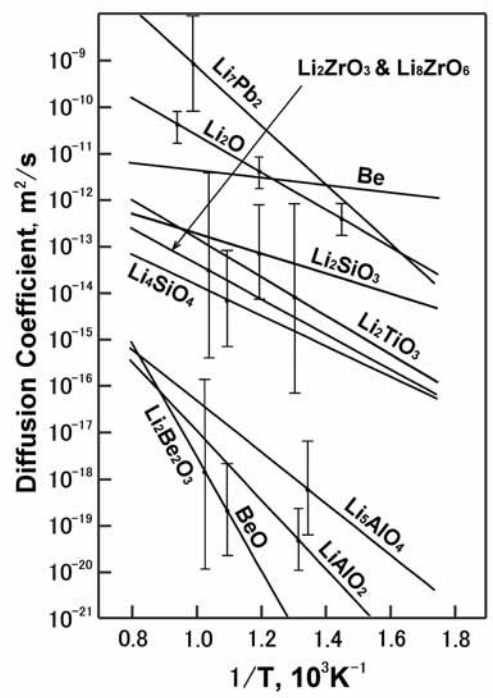

Fig.6.6 Summary of tritium diffusion coefficient in Li_2ZrO_3, Li_2O and Li_4SiO_4. [18]

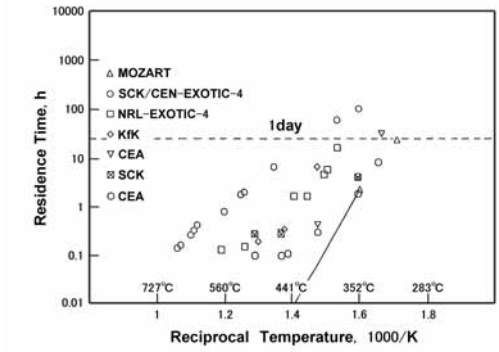

Fig.6.7 Tritium residence times for Li_2ZrO_3. [12) 47) 50)]

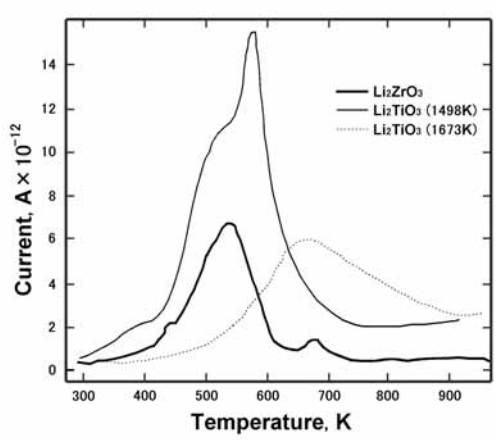

Fig.6.9 Tritium desorption curves for Li_2ZrO_3 and Li_2TiO_3 at a linear heating rate of 2 K/min., pure He sweep gas. [27]

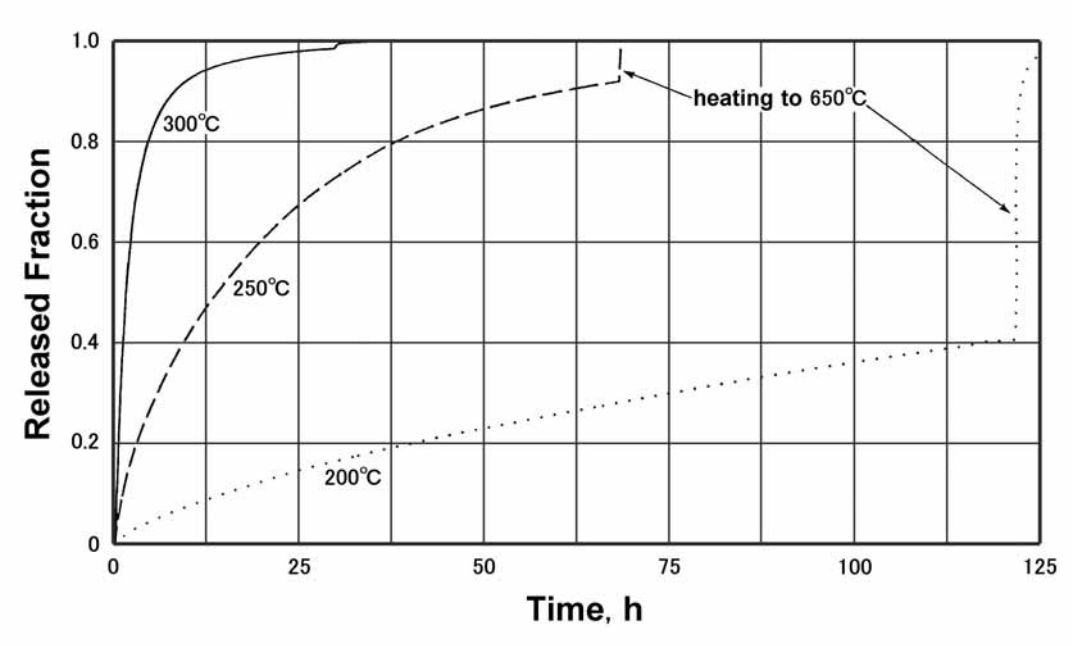

Fig.6.8 Isothermal tritium release at 300℃, 250℃, 200℃ in He + 0.1%H_2 purge gas flow rate 2.4lh^{-1} for Li_2ZrO_3. [50) 51)]

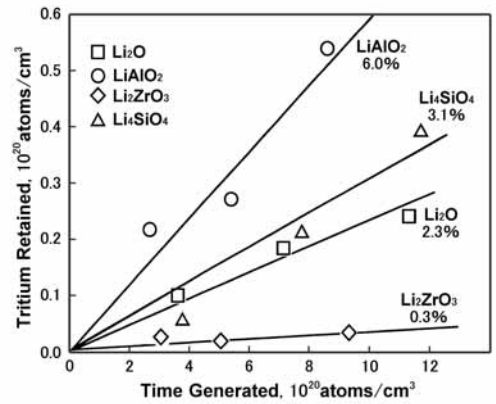

Fig.6.10 Tritium retention in Li_2ZrO_3, Li_2O and Li_4SiO_4 at 700℃. [49) 50)]

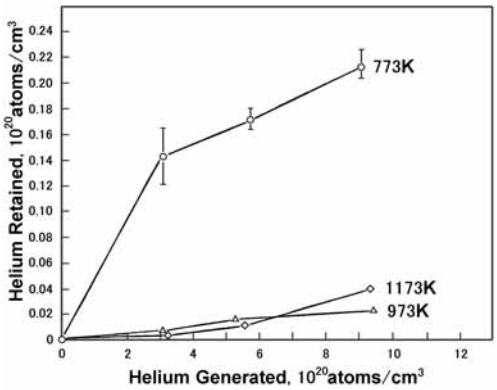

Fig.6.11 Helium retention in Li_2ZrO_3. [48)]

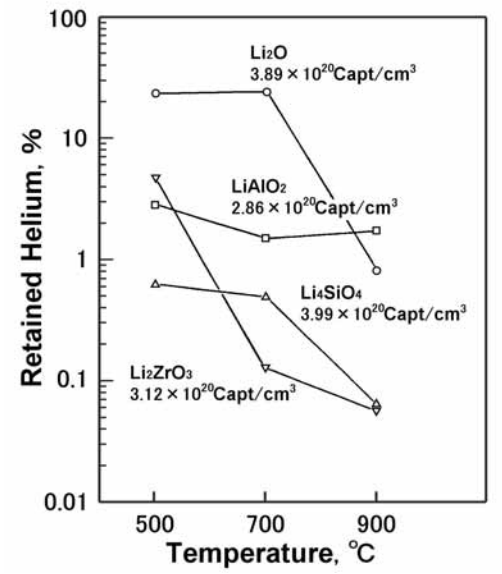

Fig.6.12 Helium retention in Li_2ZrO_3, Li_2O and Li_4SiO_4 after irradiation. [48)]

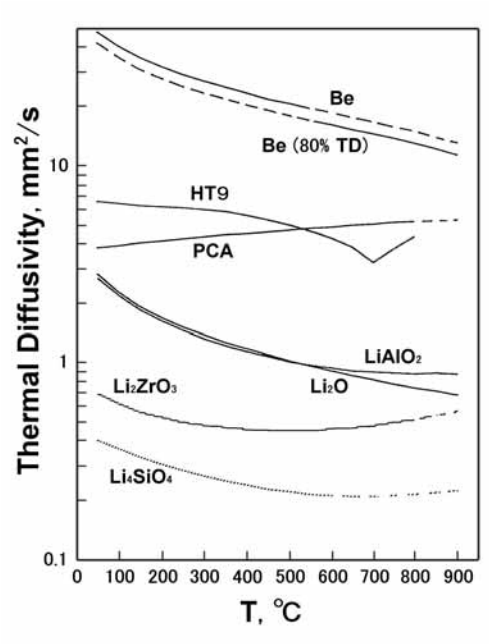

Fig.6.13 Thermal diffusivity of Li_2ZrO_3, Li_2O and Li_4SiO_4 (80% TD). [12)]